

On the character of self-interstitial dislocation loops in vanadium

L. A. ZEPEDA-RUIZ[†], J. MARIAN[‡] and B. D. WIRTH^{§*}

[†]Chemistry and Materials Science Directorate, Lawrence Livermore National Laboratory, P.O. Box 808, L-353, Livermore, CA 94550, USA

[‡]Graduate Aeronautical Laboratories, California Institute of Technology, Pasadena, CA 91125, USA

[§]Department of Nuclear Engineering, University of California, Berkeley, Berkeley, CA 94720, USA

Molecular statics and molecular dynamics simulations based on a new Finnis–Sinclair potential were used to investigate the energy and structure of self-interstitial atom (SIA) dislocation loops in vanadium. The results are compared to experimental observations and recent results in ferritic alloys which detail the formation mechanism responsible for the nucleation and growth mechanism of $\langle 100 \rangle$ dislocation loops. The SIA dislocation loops in vanadium are composed of $\langle 111 \rangle$ split dumbbells and crowdions. The clusters can be described as perfect prismatic dislocation loops with Burgers vector $\mathbf{b} = \frac{1}{2}\langle 111 \rangle$. As the loops grow, SIAs fill successive jogged-edge rows with minimum free-energy cusps corresponding tounjogged filled hexagonal shells. Notably, dislocation loops of $\langle 100 \rangle$ Burgers vector are not observed in vanadium, and these results provide a basis for understanding the experimental observations.

1. Introduction

Self-interstitial atoms (SIA) produced during collision cascades are key components of the microstructure observed when metals are irradiated with high-energy particles. The evolution of these defects may cause undesirable changes in the mechanical properties of the material under irradiation. Therefore, knowledge of the properties, formation and diffusion mechanisms of SIA is essential for understanding and predicting the effects of radiation damage.

While SiC, vanadium alloys, martensitic steels, and copper alloys are all materials of interest for the fusion program, the present study focuses on vanadium, because of its prominence in the US fusion program [1]. Vanadium exhibits an excellent combination of thermal conductivity, thermal expansion, elastic modulus, heat flux capability, compatibility with lithium, radiation swelling, and ductility.

*Corresponding author. Email: bdwirth@nuc.berkeley.edu

Extensive experimental studies of radiation damage in ferritic materials have shown the existence of prismatic dislocation loops (presumable of interstitial type) that have Burgers vectors $\mathbf{b} = \frac{1}{2}\langle 111 \rangle$, and $\mathbf{b} = \langle 100 \rangle$ in almost equal proportion [2–6]. Molecular dynamics (MD) simulations of displacement cascade evolution have revealed the formation of small mobile $\frac{1}{2}\langle 111 \rangle$ clusters with high mobility for one-dimensional motion along $\langle 111 \rangle$ orientations [7–10]. In addition, recent atomistic simulation studies in Fe have not only confirmed the stability of such loops but have also proposed a mechanism to explain the formation and growth of $\langle 100 \rangle$ loops based on the interaction on mobile $\frac{1}{2}\langle 111 \rangle$ loops [11]. In contrast to Fe, there is a lack of reliable experimental and theoretical data on defect characteristics and production in V. In fact, only a few experimental works have been carried out to examine the properties of SIA dislocation loops in vanadium. These results show the existence of dislocation loops with Burgers vector of both $\frac{1}{2}\langle 111 \rangle$ and $\frac{1}{2}\langle 110 \rangle$ type, but seldom $\langle 100 \rangle$ [2, 12].

In the present study, we employ molecular statics and molecular dynamics simulations to determine the structure and energetics of self-interstitial dislocation loops in vanadium. The results are compared to experimental observations in vanadium and dislocation loop properties in iron, and provide an explanation for the fact that $\langle 100 \rangle$ dislocation loops are not observed in vanadium.

2. Computational method

The ground-state structure and formation energy of SIA dislocation loops in vanadium, with sizes $5 \leq n \leq 127$, was investigated by molecular statics and MD simulations using a new parameterization of a Finnis–Sinclair potential for vanadium [13]. The re-parametrization was performed in order to ensure that the point defect properties were consistent with recent first-principles calculations [14] that suggest the most stable SIA is a $\langle 111 \rangle$ -dumbbell, which is nearly degenerate in energy with the crowdion configuration. This is in contrast to the case of iron, where the most stable SIA is a $\langle 110 \rangle$ -dumbbell [15]. The resultant vanadium potential has been extensively tested and successfully used in calculating point-defect properties [13, 16]. All simulations were carried out in a cubic system of size $30 a_0 \times 30 a_0 \times 30 a_0$ ($54\,000 + n$ atoms; $a_0 = 3.03 \text{ \AA}$), with periodic boundary conditions. The size of the computational cell was chosen such that strain interactions between the dislocation loops and their periodic images are negligible.

Dislocation loops of various geometries and sizes were placed at the centre of the computational cell with Burgers vectors and habit planes of $\frac{1}{2}\langle 112 \rangle\{220\}$, $\frac{1}{2}\langle 110 \rangle\{220\}$, and $\langle 100 \rangle\{220\}$. These SIA loops consisted of n successive hexagonal, rhombic or square shells (for $\frac{1}{2}\langle 111 \rangle$, $\frac{1}{2}\langle 110 \rangle$, or $\langle 100 \rangle$ loops, respectively) surrounding a central SIA. Following the insertion, a thermal structural relaxation was performed, in which the system temperature was first raised from a very low temperature ($< 1 \text{ K}$) up to 900 K. The heating schedule involves increasing the temperature in either 10 or 50 K increments with a constant heating rate of 0.005 K fs^{-1} or 0.025 K fs^{-1} for 2 ps (for $T \leq 100 \text{ K}$ and $100 < T \leq 900 \text{ K}$, respectively), followed by a hold at each temperature for 5 ps. This heating schedule was repeated until the desired temperature of 900 K was reached. Following heating schedule completion, the system was further equilibrated at 900 K for 10 ps. Finally, the system was quenched to 1 K, followed by a conjugate-gradient energy minimization to obtain the final structure and energy of the dislocation loop.

3. Results and discussion

All final configurations, obtained from the thermal structural relaxation, consisted of perfect dislocation loops with Burgers vector $\mathbf{b} = \frac{1}{2}\langle 111 \rangle$, regardless of initial configuration ($\frac{1}{2}\langle 111 \rangle\{110\}$, $\langle 110 \rangle\{110\}$, and $\langle 100 \rangle\{100\}$). These loops were highly kinked along $\langle 111 \rangle$ directions and distributed over multiple $\{220\}$ planes. A key feature observed from the MD simulations was that during the initial stage of the heating schedule ($\sim 0 \text{ K} < T < 10 \text{ K}$) initial $\frac{1}{2}\langle 110 \rangle$ or $\langle 100 \rangle$ loops reoriented almost immediately along a $\langle 111 \rangle$ direction. Then, as the heating schedule continued, these newly formed $\frac{1}{2}\langle 111 \rangle$ -oriented loops migrated very rapidly along their $\langle 111 \rangle$ glide cylinder. These results are consistent with first principles and MD simulations that showed that the most stable SIA is a $\langle 111 \rangle$ -dumbbell [13, 14, 16].

Figure 1 shows the results for the formation energy as a function of size for $\frac{1}{2}\langle 111 \rangle\{220\}$ SIA loops in V, along with the constrained formation energy for $\langle 100 \rangle\{220\}$ loops, described in more detail below. The formation energy calculated for $\frac{1}{2}\langle 111 \rangle\{220\}$ and $\langle 100 \rangle\{220\}$ loops in Fe [11] is also shown for comparison. The formation energies for the dislocation loops shown in figure 1 are listed in table 1.

We observe that $\frac{1}{2}\langle 111 \rangle$ loops are the most stable configurations for both V and Fe. Notably, Fe exhibits a metastable $\langle 100 \rangle$ configuration very close in energy to the $\frac{1}{2}\langle 111 \rangle$ loops, unlike the case in V. While the difference in formation energy between $\frac{1}{2}\langle 111 \rangle$ and $\langle 100 \rangle$ loops becomes very small ($< 10\%$) for larger loop sizes in Fe [11] it is not the case for V, where this difference increases with increasing loop size. It is important to mention that the values of the formation energy of $\langle 100 \rangle\{220\}$ loops (although thermally unstable) in V, shown in figure 1 and reported in table 1, were obtained from a constrained energy minimization where relaxation of the loop atoms was only allowed along the direction perpendicular to its Burgers vector. This was done to emphasize the much larger difference in formation energy between

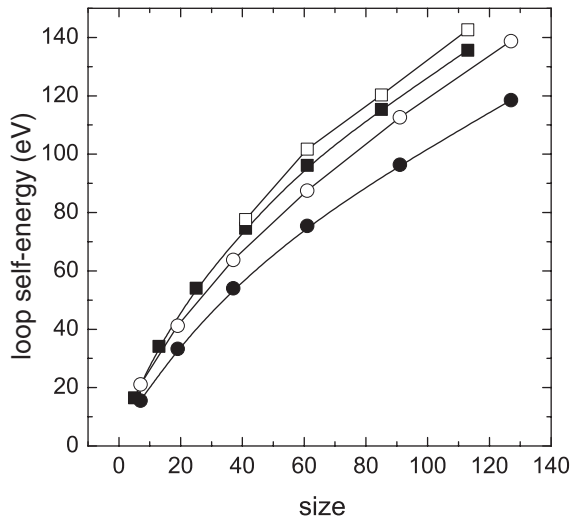


Figure 1. Dislocation loop energy as function of size (number of constituent interstitials) for $\frac{1}{2}\langle 111 \rangle\{110\}$ (●) and $\langle 100 \rangle\{110\}$ (■) loops in V and for $\frac{1}{2}\langle 111 \rangle\{110\}$ (○) and $\langle 100 \rangle\{110\}$ (□) loops in Fe [11].

Table 1. Dislocation loop energy as a function of size (number of constituents interstitials) and orientation for SIA loops in V and in Fe [11].

	7	19	37	61	91	127	
V $\frac{1}{2}\langle 111\rangle\{110\}$	15.57	33.26	54.00	75.42	96.31	118.5	
Fe $\frac{1}{2}\langle 111\rangle\{110\}$	21.08	41.24	63.79	87.56	112.6	138.8	
	5	13	25	41	61	85	113
V $\langle 100\rangle\{110\}$	16.50	34.12	54.10	74.58	96.15	115.4	135.6
Fe $\langle 100\rangle\{110\}$	–	–	–	77.60	101.7	120.3	142.6

$\frac{1}{2}\langle 111\rangle$ and $\langle 100\rangle$ loops in V than in Fe and, thus, provide a partial explanation as to why the $\langle 100\rangle$ loops are not observed experimentally in V.

Recent MD simulations by Marian *et al.* [11] have shown that a possible mechanism for the formation and growth of $\langle 100\rangle$ dislocation loops in Fe involves reactions between $\frac{1}{2}\langle 111\rangle$ -type loops of the type



They showed that when two loops, of comparable sizes, intersect according to equation (1), a stable $\langle 100\rangle$ junction is formed. Given sufficient time, this junction propagates throughout the loops via a multiple-step process that results in the ultimate growth of the $\langle 100\rangle\{100\}$ junction until the whole loop is transformed. The resulting $\langle 100\rangle$ loops are metastable, practically immobile, and grow by direct absorption of smaller clusters [11].

In order to shed light onto the absence of $\langle 100\rangle$ loop formation in V by this mechanism, we performed MD simulations of interactions between $\frac{1}{2}\langle 111\rangle$ loops. These simulations were carried out in a supercell containing 54 000 lattice sites and two hexagonal loops with Burgers vectors according to equation (1). Initially, the two loops are thermalized at low temperatures (~ 50 K) and subsequently brought to a target temperature of 600 K with the heating schedule explained in the previous section. At this temperature the defects undergo annealing in the microcanonical ensemble. The two loops are forced to interact with each other by ensuring that their respective glide prisms intersect in space.

Figure 2 shows a sequence of snapshots from the MD simulation. Figure 2a shows two hexagonal loops of sizes $n = 19$ and 16 with Burgers vector $\mathbf{b} = \frac{1}{2}\langle 111\rangle$ and $\mathbf{b} = \frac{1}{2}\langle 1\bar{1}\bar{1}\rangle$, respectively. During annealing at 600 K, the two loops glide towards each other and collide, driven by the energy reduction when two loops condense into a single loop. Immediately after the collision, a very small $\langle 100\rangle$ junction (1–3 SIAs) is formed, as shown in figure 2b). At this temperature (600 K), the junction oscillates between the Burgers vectors of the two starting dislocation loops. To test the thermal stability of the $\langle 100\rangle$ junction, we performed isochronal annealing up to 900 K with a heating rate of 0.01 K fs $^{-1}$. During isochronal annealing, the $\langle 100\rangle$ junction proved to be unstable. Ultimately, the smaller dislocation loop (16 SIAs) rotated and was absorbed by the larger one (19 SIAs), adopting its Burger vector. The result of this transformation is a single, larger, loop with final Burgers vector $\mathbf{b} = \frac{1}{2}\langle 111\rangle$, as shown in figure 2c. A more detailed description of the loop rotation mechanism will be the subject of a further publication. The interaction of larger $\frac{1}{2}\langle 111\rangle$ clusters of the same size (both clusters containing 37 SIA) also did not reveal the formation

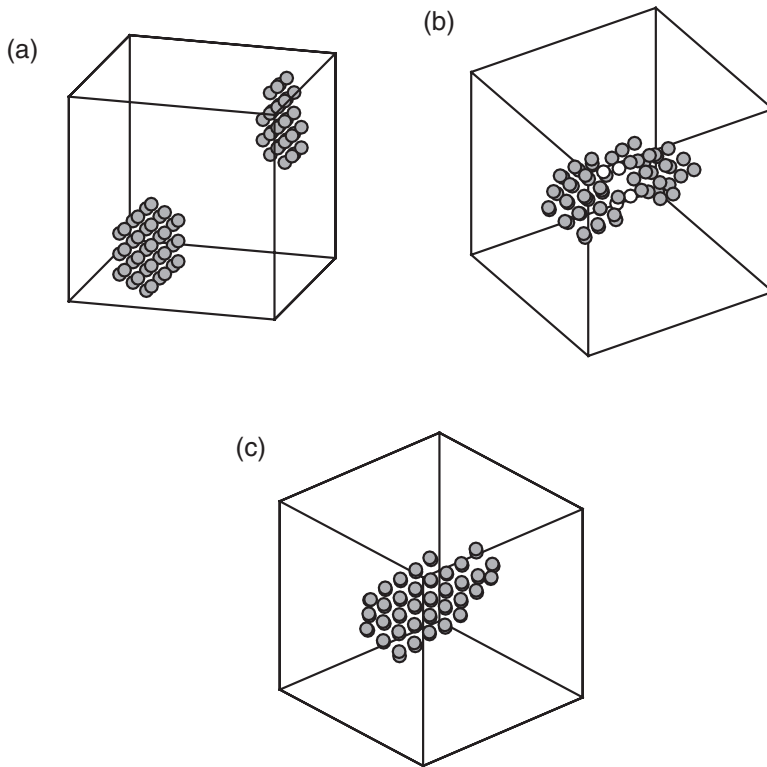


Figure 2. Sequence of MD snapshots at (a) 0, (b) 50, and (c) 85 ps, of the interaction of two $\frac{1}{2}\langle 111 \rangle$ with Burgers vectors according to equation (1). The atoms forming the $\langle 100 \rangle$ junction are coloured white for clarity.

of large $\langle 100 \rangle$ junction. In this case, the two loops interact and form a small unstable $\langle 100 \rangle$ junction (3–5 SIAs), that quickly rotated between $\langle 11\bar{1} \rangle$ and $\langle \bar{1}11 \rangle$ orientations. During longer simulation times (100 ps), neither of the loops re-oriented to form a single $\langle 111 \rangle$ loop and remained self-trapped, although notably without the existence of a $\langle 100 \rangle$ junction.

4. Summary and conclusions

We have used an improved Finnis–Sinclair potential for vanadium [13], fit to first-principles calculations of point defect properties [14], to investigate the characteristics of self-interstitial clusters. SIA dislocation loops with $\frac{1}{2}\langle 111 \rangle$ Burgers vector are the lowest energy configuration in vanadium, and migrate rapidly along their $\langle 111 \rangle$ glid cylinder. Initial dislocation loop configurations with Burgers vector of $\frac{1}{2}\langle 110 \rangle$ or $\langle 100 \rangle$ rotated into $\frac{1}{2}\langle 111 \rangle$ orientations at very low temperatures during the computational relaxation scheme used in this work and indicate that the formation energy of $\frac{1}{2}\langle 110 \rangle$ and $\langle 100 \rangle$ loops is much higher than $\frac{1}{2}\langle 111 \rangle$ loops. Unlike in Fe, where a metastable $\langle 100 \rangle$ loop is very close in energy to the ground-state $\frac{1}{2}\langle 111 \rangle$ orientation, constrained $\langle 100 \rangle$ loops in V have considerably higher formation energies than $\frac{1}{2}\langle 111 \rangle$ loops, and the energy difference increases with size.

MD simulations of the interaction between two mobile $\frac{1}{2}\langle 111 \rangle$ clusters, according to the reaction proposed for $\langle 100 \rangle$ loop formation in Fe [11], reveal the formation of a single resulting $\frac{1}{2}\langle 111 \rangle$ loop. The simulations indicate that while the reaction occurs (a $\langle 100 \rangle$ -junction does form), the junction has a very low thermal stability and rotates into a $\langle 111 \rangle$ orientation at temperatures of 600–800 K. The simulations performed to date provide no indication that the smaller $\langle 100 \rangle$ junctions will propagate across the loop, but instead will dissolve with low thermal stability.

Acknowledgements

This work was performed under the auspices of the U.S. Department of Energy by the University of California, Lawrence Livermore National Laboratory under Contract No. W-7405-Eng-48.

References

- [1] H.M. Chung, B.A. Loomis and D.L. Smith, *J. Nucl. Mater.* **239** 139 (1996).
- [2] D.S. Gelles, P.M. Rice, S.J. Zinkle, *et al.*, *J. Nucl. Mater.* **258–263** 1380 (1998).
- [3] A.E. Ward and S.B. Fisher, *J. Nucl. Mater.* **166** 227 (1989).
- [4] B.C. Masters, *Phil. Mag.* **11** 881 (1965).
- [5] E.A. Little, R. Bullough and M.H. Wood, *Proc. R. Soc. Lond. A* **372** 565 (1980).
- [6] A.C. Nicol, M.L. Jenkins and M.A. Kirk, *Mater. Res. Soc. Symp.* **650** R1.3 (2001).
- [7] Y.N. Osetsky, A. Serra, B.N. Singh, *et al.*, *Philos. Mag. A* **80** 2131 (2000).
- [8] D.J. Bacon and T. Díaz de la Rubia, *J. Nucl. Mater.* **216** 275 (1994).
- [9] N. Soneda and T. Díaz de la Rubia, *Philos. Mag. A* **78** 995 (1998).
- [10] R.E. Stoller, *J. Nucl. Mater.* **233–237B** 999 (1996).
- [11] J. Marian, B.D. Wirth and J.M. Perlado, *Phys. Rev. Lett.* **88** 255507 (2002).
- [12] P.M. Rice and S.J. Zinkle, *J. Nucl. Mater.* **158–163** 1414 (1998).
- [13] S. Han, L.A. Zepeda-Ruiz, G.J. Ackland, *et al.*, *J. Appl. Phys.* **93** 3328 (2003).
- [14] S. Han, L.A. Zepeda-Ruiz, G.J. Ackland, *et al.*, *Phys. Rev. B* **66** 220101–1 (2002).
- [15] B.D. Wirth, G.R. Odette, D. Maroudas, *et al.*, *J. Nucl. Mater.* **244** 185 (1997).
- [16] L.A. Zepeda-Ruiz, S. Han, R. Car, *et al.*, *Phys. Rev. B* **67** 134114-1 (2003).